Cytotechnology (2004) 46:9–18
DOI 10.1007/s10616-005-1476-5

Identification of three gene candidates for multicellular resistance in colon carcinoma

Nicholas E. Timmins[1], Tina L. Maguire[2], Sean M. Grimmond[2] & Lars K. Nielsen[1,*]
[1]*Laboratory for Biological Engineering, Department of Chemical Engineering, University of Queensland, Brisbane, QLD, Australia;* [2]*The Institute for Molecular Biosciences, The University of Queensland, Brisbane, QLD 4072, Australia (*Author for correspondence; E-mail: lars.nielsen@uq.edu.au; phone: +61-7-3365-4682; fax: +61-7-3365-4199)*

Received 3 June 2004; accepted in revised form 21 January 2005

Key words: 3D culture, Differential gene expression, MCR, MCS, Multicellular resistance, Multicellular spheroid, Tumour

Abstract

Solid tumours display elevated resistance to chemo- and radiotherapies compared to individual tumour derived cells. This so-called multicellular resistance (MCR) phenomenon can only be partly explained by reduced diffusion and altered cell cycle status; even fast growing cells on the surface of solid tumours display MCR. Multicellular spheroids (MCS) recapture this phenomenon *ex vivo* and here we compare gene expression in exponentially growing MCS with gene expression in monolayer culture. Using an 18,664 gene microarray, we identified 42 differentially expressed genes and three of these genes can be linked to potential mechanisms of MCR. A group of interferon response genes were also up-regulated in MCS, as were a number of genes that that are indicative of greater differentiation in three-dimensional cultures.

Abbreviations: 3D – Three-dimensional; 5FU – 5-Fluorouracil; MCR – Multicellular resistance; MCS – Multicellular spheroid

Introduction

Promising new anti-cancer agents identified using *in vitro* monolayer cultures of tumour derived cells often fail *in vivo*. Compared to mono-layer cell cultures, solid tumours are more resistant to anti-cancer therapies that directly target the malignant cell population. This phenomenon is known as multicellular resistance (MCR) (Desoize and Jardillier 2000). MCR is also observed in MCS, which as a result have been heralded as an excellent *in vitro* model with which to study tumours and identify, test, and develop new therapies (Sutherland 1988; Mueller-Klieser 1997; Hamilton 1998; Kunz-Schughart et al. 1998; Desoize and Jardillier 2000; Dubessy et al. 2000; Fracasso and Colombatti 2000). These cellular aggregates recapture the microenvironmental conditions that exist within avascular tumour regions and micrometastases, leading to the development of heterogeneous cell populations and an overall phenotype that mimics that observed *in vivo*.

Early explanations of the MCR effect were largely based on the nature of the cellular environment that arises in solid tissues. Poor perfusion of avascular tumour/MCS regions leads to

poor transport of drugs into the tumour, while reduced oxygen levels contribute to radio-resistance. Consideration of cell cycle status also explained some of the MCR effect, quiescent cells within the tumour/MCS being less susceptible to those agents targeting cellular proliferation. However, this cannot explain the observation that small MCS of only 25–50 cells, and cells from the outer layers of MCS, also exhibit a resistant phenotype (Olive and Durand 1994). Furthermore, this resistance is retained for a period after dissociation of cells from the MCS (Olive et al. 1993; Olive and Durand 1994). Such observations suggest that fundamental changes in the nature of cells growing as 3D tissue constructs must, at least in part, be responsible for the observed effects of MCR.

Compared to monolayers a variety of changes to cellular phenotype take place in 3D culture (e.g. changes to chromatin packing and cell size/shape (Olive and Durand 1994; Desoize and Jardillier 2000), changes in sub-cellular protein localisation (Oloumi et al. 2000), differential expression of adhesion molecules (Rainaldi et al. 1999; Shiras et al. 2002), resistance to apoptosis (Desoize and Jardillier 2000), increased expression of multidrug resistance related proteins (Wartenberg et al. 1998; Desoize and Jardillier 2000) and broader changes in protein expression (Poland et al. 2002), and these in turn result in, or are the result of, altered gene expression (Olive and Durand 1994; Knowles and Phillips 2001; Oloumi et al. 2002).

Only two investigations into broad changes in gene expression between monolayers and MCS have been undertaken (Knowles and Phillips 2001; Oloumi et al. 2002), and these have identified a small number of differentially regulated genes. However, in consideration of the number of reports describing differential expression of specific genes and gene products, the true extent to which gene expression differs between MCS and monolayers is expected to be much greater.

We demonstrate that MCS generated from human colon carcinoma derived cells exhibit an MCR phenotype that cannot be easily explained by diffusion limitations and quiescent cell populations. These MCS differentially express 42 genes compared to monolayers, and based on known functions three of these can be linked with possible mechanisms of MCR. A number of interferon response and differentiation related genes are also differentially expressed, as are a group of genes that are also differentially expressed in tumours compared to healthy tissues.

Materials and methods

Monolayer cell culture

HCT116 colon carcinoma cells were routinely cultivated as monolayers in DMEM medium (GibcoBRL) supplemented with 10% foetal bovine serum (JRH Biosciences) in a 5% CO_2, humidified atmosphere at 37 °C. Cell enumeration was achieved using an improved Neubauer haemocytometer and trypan blue exclusion.

Multicellular spheroid culture

HCT116 MCS were cultivated by the hanging drop method as previously described (Kelm et al. 2003). Twenty microlitres of single cell suspension were dispensed into the wells of a 60-well mini tray (Nunc), giving 100 cells/well. Trays were inverted, placed inside larger bio-assay trays, and incubated as above.

Analysis of multicellular spheroid growth kinetics

Images for kinetic analysis of MCS ($n = 50$) were captured at the desired times using an Olympus BX61 microscope fitted with a Cool-Snap *cf* Pro CCD camera (MediaCybernetics) and subsequently analysed for size and roundness (1 = perfectly round) using ImagePro Plus 4.5 (MediaCybernetics).

Sectioning and staining

MCS for histological sectioning were harvested on day 8 and fixed in 3.7% formaldehyde solution for 10 min. They were then rinsed with PBS and suspended in 30% sucrose solution (in PBS until) the MCS had sunk to the bottom of the tube, at which point OCT (TissueTek) was added and mixed, suspending the MCS in a 1:1 OCT: sucrose solution. This was then left overnight at room

temperature. Samples were transferred to moulds, embedded in OCT, and stored at −80 °C until sectioning. Frozen sections were obtained using a Leitz cryo-microtome, and transferred to Super-Frost Plus glass slides. Staining was achieved using Mayers hematoxylin (Sigma) and Eosin Y (Sigma).

Response to 5-fluorouracil exposure

Day 8 (approximately 300 μm in diameter) MCS were harvested in PBS and transferred in approximately equal numbers to polystyrene dishes. To these MCS and T25 monolayer cultures, 100 μg/ml 5-Fluorouracil (5FU) was added in fresh DMEM growth medium, and incubated as above.

At the desired times, monolayer cultures were trypsinised and resuspended in an appropriate volume of serum free DMEM. MCS were dissociated by incubation in 0.05% EDTA in PBS for 20 min at 37 °C, followed by 5 min in 0.25% trypsin and aspiration with a 21 g needle. Cell viability for each sample was determined using a Molecular Probes Live/Dead assay kit. Sixty fields of a haemocytometer chamber were captured using the aforementioned microscopy system, and images were processed using ImagePro Plus 4.5 to identify the number of viable and non-viable cells in each. These data were then transferred to MS Excel and the % viability calculated.

Microarray profiling

The arrays used in this study were obtained from the SRC Microarray Facility, University of Queensland (ARC Centre for Functional and Applied Genomics), and comprised 18,664 (excluding controls) human gene-specific oligonucleotides (Compugen) spotted onto epoxy-silane coated sides (Eppendorf creative slides).

Total RNA was isolated from MCS (day 8) and monolayer cultures using a QIAGEN RNeasy purification kit. RNA quality and quantity were assessed using a Bioanalyser RNA6000 NanoAssay (Agilnet). Two micrograms of each total RNA sample were amplified using an Ambion Amino Allyl Messageamp^{TM} aRNA Kit. Amplified RNA was labelled using indirect cy3/cy5 incorporation (Ambion). Hybridisations were performed in duplicate and incorporated a dye swap to account for dye bias. After 16 h hybridisation, the arrays were washed and scanned on an Agilnet 61565BA microarray scanner at a 5 μm resolution.

The resulting images were analysed using Imagene 5.5 (Biodiscovery) and the mean foreground, background and spot/signal quality determined. Data were then exported into Genespring 6.1 (Silicon Genetics) and the mean differential expression was observed. A further filtering of data with a mean intensity of at least 300 fluorescence units was included. Finally, elements with ≥ 2-fold change in expression between MCS and monolayers were identified.

Real-time PCR

Confirmation of differential gene expression for select genes was achieved through relative quantitation by real-time PCR using an Applied Biosystems ABI Prism 7000 sequence detection system and SYBR green (Applied Biosystems).

Total RNA was extracted from MCS and monolayer cultures as described above. RNA was DNase (Fermentas) treated, and cDNA generated by reverse transcription using Superscript III (Invitrogen) according to the manufacturers instructions. Primers were designed using Primer Express v2.0 (Applied Biosystems) and were purchased from Sigma Genosys (Table 1).

Real-time PCR product identity was confirmed by melt curve analysis and 2% agarose gel

Table 1. Primers employed for real-time PCR.

Gene	Forward primer	Reverse primer
S100A4	CGCTTCTTCTTTCTTGGTTTGATC	ATCACATCCAGGGCCTTCTC
SKIP3	CTGGCATCCTTGAGCTGACA	GGCCGACACTGGTACAAAGTG
p48	CGGAGTGTGCTGGGATGATA	CCTGCTTGCCTGCATGTTT
STAT1	TCTAGACTTCAGACCACAGACAACCT	CAGAGCCCACTATCCGAGACA
GAPDH	GAAGATGGTGATGGGGATTTC	GAAGGTGAAGGTCGGAGT

electrophoresis. Absence of genomic DNA was confirmed in minus RT controls. No template controls were included in each run. Cycle thresholds were determined using ABI Prism 7000 SDS v1.1 software (Applied Biosystems) and efficiencies calculated by a log-linear fit to points either side of the threshold fluorescence value using LinReg v7.5 (Ramakers et al. 2003). Data were normalised to GAPDH and the change in expression between MCS and monolayers was expressed as the ratio of these values. All data were collected in triplicate and errors calculated by propagation and expressed as the standard deviation in fold change.

Results

Growth characteristics of HCT116 multicellular spheroids (MCS)

HCT116 MCS cultivated by the hanging drop method display a typical Gompertz type growth pattern (Marusic et al. 1994; Lazareff et al. 1999; Kunz-Schughart and Mueller-Klieser 2000), with an exponential increase in volume between days 3 and 9, followed by a decline in growth rate and subsequent plateau phase (Figure 1). This is paralleled by a decreasing roundness factor, indicating greater sphericity as cells coalesce and the MCS develops. MCS of approximately 300 μm diameter (day 8) showed no obvious signs of extensive central apoptosis or necrosis in histological sections (Figure 2).

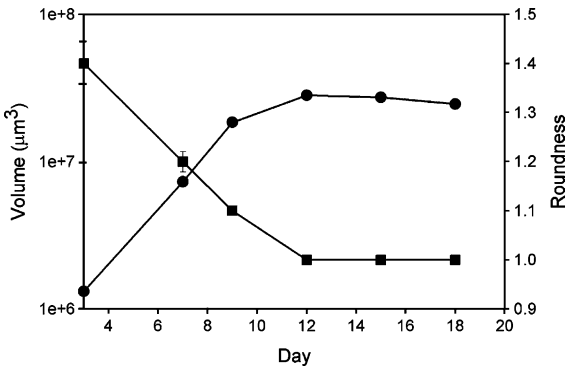

Figure 1. Growth kinetics of HCT116 MCS (volume – circle, roundness – square, $n = 50$). Cells aggregate and grow exponentially through to day 9, followed by a decline in growth rate and eventual plateau. Error bars depict standard error of the mean.

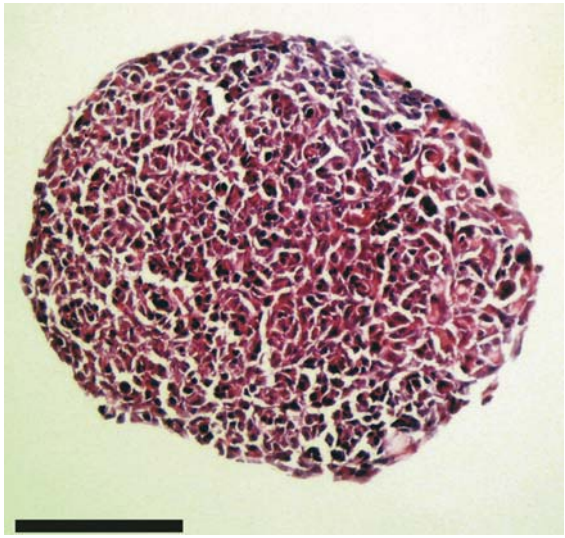

Figure 2. Hematoxylin and eosin stained cryosection of a day 8 MCS. No obvious signs of extensive apoptosis or necrosis in central regions are evident. Bar = 100 μm.

Response to 5-fluorouracil exposure

Upon exposure to 100 μg/ml 5FU, MCS show reduced sensitivity compared to monolayer cell cultures. At 120 h, $58 \pm 1.9\%$ of monolayer cells were no longer viable, compared to $31 \pm 1.6\%$ of cells from MCS (Figure 3). The method employed for viability counting circumvented issues of incomplete dissociation of MCS leading to small cell clusters. These clusters were a constant source of problems when using flow cytometric analysis, and further trypsination was considered overly harsh. Using image analysis it was possible to identify individual cells within small clusters. A slightly higher initial dead cell count for MCS most likely reflects membrane damage caused during dissociation.

The use of MCS in the exponential phase (day 8) implies that if present, the quiescent cell population is small and does not represent a significant fraction of the total population, minimising the size of this resistant population.

Differential gene expression

Microarray profiling was used to identify genes differentially expressed in MCS compared to monolayers (Figure 4). Data revealed 42 transcripts

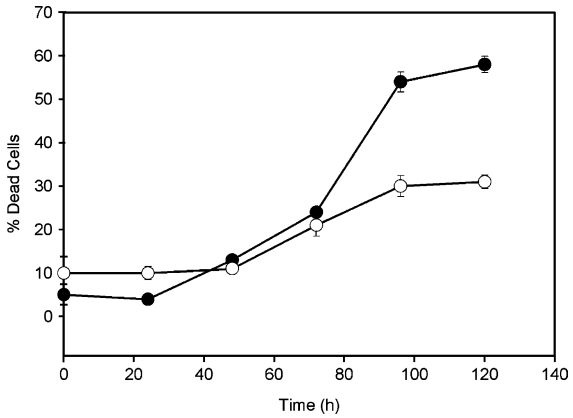

Figure 3. Viability of HCT116 cultures exposed to 100 μg/ml 5FU (monolayer – closed circle, MCS – open circle). After 120 h, 27% more dead cells are observed in monolayer cultures. A slightly higher initial percentage of dead cells in MCS cultures most likely reflects damage caused during dissociation. Error bar depict standard error of the mean.

differentially expressed by more than 2-fold (Table 2), three of these can be linked to potential mechanisms of MCR, 13 are involved in interferon response, 10 are differentiation related, and 14 are differentially regulated in tumours compared to healthy tissue. A further 17 differentially expressed genes were also identified. The use of MCS approximately 300 μm in diameter (exponential growth and absence of an apoptotic/necrotic core) should limit the extent of changes occurring in gene expression arising as a result of extreme environmental conditions (e.g. hypoxia response genes), changes in proliferate status (e.g. cell cycle regulators), and changes in cellular viability (e.g. apoptosis machinery), highlighting those genes differentially regulated in as a result of 3D architecture.

From a search of the available literature and gene databases, three genes were identified as candidate MCR related genes, and the differential expression of these genes (*S100A4*, *SKIP3* and *p48*) verified by real-time PCR. Due to its position at the top of the interferon response signalling pathway and the high number of differentially regulated interferon response related genes identified, the differential expression of *STAT1* was also verified by real-time PCR (Table 3).

Discussion

Tumours and MCS exhibit enhanced resistance to anti-cancer agents compared to monolayer cultures (Nederman and Twentyman 1984; Mueller-

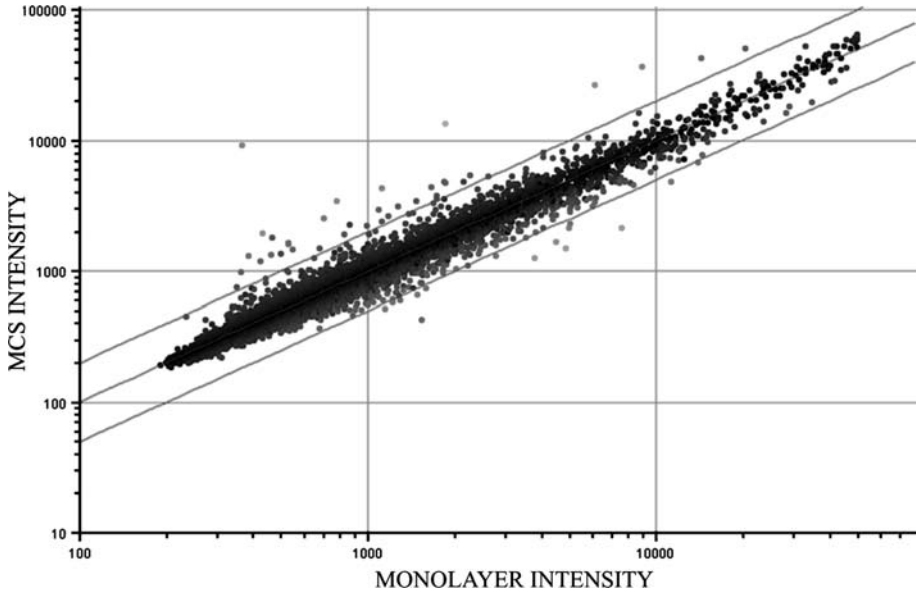

Figure 4. Scatter plot of average spot signal intensities from 18,664 gene microarrays. Outer diagonal lines represent a 2-fold change in signal intensity. Array hybridisations were performed in duplicate and incorporated a dye swap. Although shown above, spots with a signal intensity of less than 300 were excluded from further analysis.

Table 2. Genes differentially expressed by more than 2-fold (microarray) in HCT116 MCS compared to monolayers grouped by known function.

Gene name	LocusLink	Ontology	Expression ratio
MCR related			
Interferon-stimulated transcription factor 3, gamma 48 kDa (*p48*)	10,379	Transcription regulation	2.4 ± 0.46
S100 calcium binding protein A4 (calcium protein, calvasculin, metastasin - *S100A4*)	6275	Signal transduction	3.0 ± 0.32
Chromosome 20 open reading frame 97 (*SKIP3*)	57,761	Protein amino acid phosphorylation	0.29 ± 0.033
Interferon response			
Signal transducer and activator of transcription 1, 91 kDa (*STAT1*)	6772	JAK-STAT cascade	2.0 ± 0.61
Melanoma differentiation associated protein-5	64,135	RNA processing	3.0 ± 0.65
2′,5′-oligoadenylate synthetase 1, 40/46 kDa	4938	Immune response	2.7 ± 0.34
Interferon-stimulated transcription factor 3, gamma 48 kDa	10,379	Transcription regulation	2.4 ± 0.46
Ubiquitin specific protease 18	11,274	Ubiquitin-dependent protein degradation	3.6 ± 0.45
N-myc (and STAT) interactor	9111	JAK-STAT Cascade	2.7 ± 0.37
Interferon, alpha iducible protein (clone IFI-6–16)	2537	Immune response	4.5 ± 0.86
Interferon, alpha inducible protein (clone IFI-15K)	9636	Polyubiquitylation	4.0 ± 0.72
Proteasome (prosome, macropain) subunit, beta type, 9 (large multifunctional protease 2)	5698	Proteolysis and peptidolysis	2.9 ± 0.40
Interferon-induced protein 35	3430	Immune response	2.2 ± 0.25
Protein kinase, interferon-inducible double stranded RNA dependent	5610	Protein amino acid phosphorylation	2.5 ± 0.27
Regulator of G-protein signalling 2, 24 kDa	5997	Regulation of G-protein coupled receptor protein signaling pathway	2.2 ± 0.42
Retinoic acid- and interferon-inducible protein (58 kDa)	24,138	Immune response	2.0 ± 0.56
Differentiation			
S100 calcium binding protein A4 (calcium protein, calvasculin, metastasin)	6275	Signal transduction	2.3 ± 0.32
Signal transducer and activator of transcription 1, 91 kDa	6772	JAK-STAT cascade	2.0 ± 0.61
Melanoma differentiation associated protein-5	64,135	RNA processing	3.0 ± 0.65
2′,5′-oligoadenylate synthetase 1, 40/46 kDa	4938	Immune response	2.7 ± 0.34
Interferon-stimulated transcription factor 3, gamma 48 kDa	10,379	Transcription regulation	2.4 ± 0.46
Tetraspan 1	10,103	Cell adhesion	2.3 ± 0.21
Visinin-like 1	7447	Central nervous system development	2.5 ± 0.57
Ets homologous factor	26,298	Biological process unknown	2.4 ± 0.64
Dual specificity phosphatase 1	1843	Biological process unknown	0.46 ± 0.05
Cystatin A (stefin A)	1475	Embryogenesis and morphogenesis	0.48 ± 0.012

Differentially expressed in tumours vs. healthy tissue			
Transcobalamin I (vitamin B12 binding protein, R binder family)	6947	Cobalt ion transport	2.8 ± 0.53
Interferon-stimulated transcription factor 3, gamma 48 kDa	10,379	Transcription regulation	2.4 ± 0.46
Tetraspan 1	10,103	Cell adhesion	2.3 ± 0.21
Visinin-like 1	7447	Central nervous system development	2.5 ± 0.57
Ets homologous factor	26,298	Biological process unknown	2.4 ± 0.64
Proteasome (prosome, macropain) subunit, beta type, 9 (large multifunctional protease 2)	5698	Proteolysis and peptidolysis	2.9 ± 0.40
Secreted and transmembrane 1	6398	Immune response	3.9 ± 0.87
Protein kinase, interferon-inducible double stranded RNA dependent	5610	Protein amino acid phosphorylation	2.5 ± 0.27
Regulator of G-protein signalling 2, 24 kDa	5997	Regulation of G-protein coupled receptor protein signalling pathway	2.2 ± 0.42
S100 calcium binding protein A4 (calcium protein, calvasculin, metastasin)	6275	Signal transduction	3.0 ± 0.32
Dual specificity phosphatase 1	1843	Biological process unknown	0.46 ± 0.05
Cystatin A (stefin A)	1475	Embryogenesis and morphogenesis	0.48 ± 0.0012
Chromosome 20 open reading frame 97	57,761	Protein amino acid phosphorylation	0.29 ± 0.033
Highly expressed in cancer, rich in leucine heptad repeats	10,403	Mitotic chromosome segregation	0.46 ± 0.010
Other			
Hypothetical protein FLJ20073	54,809	Biological process unknown	2.9 ± 0.30
Heparin-binding growth factor binding protein	9982	Signal transduction	3.1 ± 0.15
Rhysin 2	151,636	Biological process unknown	4.4 ± 0.41
Sarcoglycan, gamma (35 kDa dystrophin-associated glycoprotein)	6445	Muscle development	2.2 ± 0.13
LIM domain only 2 (rhombotin-like 1)	4005	Developmental processes	2.3 ± 0.50
Sterol-C4-methyl oxidase-like	6307	Ergosterol biosynthesis	2.2 ± 0.29
Ubiquitin-conjugating enzyme E2L 6	9246	Protein modification	2.0 ± 0.37
Cytosolic sialic acid 9-*O*-acetylesterase homolog	54,414	Cell death	2.6 ± 0.43
Coactosin-like 1 (Dictyostelium)	23,406	Biological process unknown	0.50 ± 0.12
Phosphoserine aminotransferase 1	29,968	Methionine metabolism	0.46 ± 0.069
Short-chain dehydrogenase/reductase 1	9249	Nitrogen metabolism	0.47 ± 0.12
Asparagine synthetase	440	Asparagines biosynthesis	0.33 ± 0.066
Methionine-tRNA synthetase	4141	Cell cycle control	0.35 ± 0.091
Uridine phosphorylase 1	7378	Nucleobase, nucleoside, nucleotide and nucleic acid metabolism	0.30 ± 0.11
Glycyl-tRNA synthetase	2617	Protein biosynthesis	0.42 ± 0.061
Cysteinyl-tRNA synthetase	833	Protein biosynthesis	0.44 ± 0.073
Tyrosyl-tRNA synthetase	8565	Apoptosis	0.48 ± 0.067

Expression ratio is for MCS compared to monolayer (± standard deviation), gene ontology according to Compugen.

Table 3. Fold change in expression of MCR related genes as determined by real-time PCR, multicellular spheroid vs. monolayer (± standard deviation).

Gene	Expression ratio
p48	4.4 ± 0.53
S100A4	2.3 ± 0.33
SKIP3	0.41 ± 0.06
STAT1	1.8 ± 0.22

Klieser 1997; Hamilton 1998; Kunz-Schughart et al. 1998; Dubessy et al. 2000; Fracasso and Colombatti 2000), and this resistance cannot be fully explained by microenvironmental conditions or the existence of quiescent cell populations (Olive et al. 1993; Olive and Durand 1994; Desoize and Jardillier 2000).

When small (approximately 300 μm diameter) exponentially growing HCT116 colon carcinoma MCS (Figure 1) and monolayer cultures were continuously exposed to 5FU, a significant difference in cellular viability was observed after 120 h (31% vs. 58% respectively; Figure 3). As 5FU penetrates rapidly into MCS (Nederman and Twentyman 1984), diffusion limitations cannot account for the reduced killing effect. Similarly, the use of MCS in the exponential growth phase excludes resistance arising from quiescent cell populations.

Changes in the expression of various genes and proteins are known to occur in 3D culture (Olive and Durand 1994; Knowles and Phillips 2001; Oloumi et al. 2002; Poland et al. 2002) and it is thought that these also contribute to the MCR phenotype. We employed microarray technology to examine the extent to which such changes in gene expression occur between the above cultures, and if these changes can be linked to possible mechanisms of MCR based on their known functions.

In total, we identified 42 genes differentially expressed by more than 2-fold in HCT116 MCS compared to monolayer cultures (Table 2). Of these 42 genes, a review of available literature suggested that three of these might contribute to the MCR phenotype (*S100A4*, *SKIP3*, and *p48*), and the change in expression of these genes was evaluated by real-time PCR (Table 3).

Up-regulation of S100A4 (calcium binding) in MCS has previously been identified at both the transcript and protein level (Oloumi et al. 2002), and in tumours increased expression correlates with an invasive, metastatic phenotype (Rosty et al. 2002; Flatmark et al. 2003; Moriyama-Kita et al. 2004). Oloumi et al. (2002) showed that S100A4 expression is up-regulated in V79 and C6 MCS, and that both are resistant to etoposide treatment. Hypothesising that this was due to differences in free intracellular calcium levels as a result of S100A4 activity, they treated monolayer cultures with the calcium chelating agent BAPTA-AM. When subsequently exposed to etoposide, monolayers treated with BAPTA-AM were found to be less sensitive to this drug, exhibiting decreased levels of DNA damage similar to that observed for MCS. We have also observed the up-regulation of *SI00A4* (2.3-fold) in HCT116 MCS, while others have identified the up-regulation of additional calcium binding proteins in other cell lines (Knowles and Phillips 2001; Oloumi et al. 2002; Poland et al. 2002). The underlying reasons for the increased expression of calcium binding proteins remain unknown, but available data suggest that this may be a common feature of 3D cultures and might contribute to the MCR phenotype.

The second gene of relevance to the MCR, phenotype is *SKIP3* (down-regulated 2.4-fold in MCS). *SKIP3* is an NF-κB inducible gene, and a negative feed back inhibitor of NF-κB dependent gene expression (Wu et al. 2003) NF-κB is known to confer resistance to cytotoxic therapies via suppression of apoptosis, and its transcriptional activity is regulated by phosphorylation of the p65 subunit (Mayo and Baldwin 2000; Baldwin 2001; Weaver et al. 2002; Huang et al. 2003; Debatin 2004). SKIP3 inhibits p65 phosphorylation by PKAc, reducing the transcriptional activity of NF-κB, and consequently sensitises cells to apoptosis (Wu et al. 2003). A decrease in *SKIP3* expression in HCT116 MCS might contribute to the MCR phenotype by reducing feedback inhibition of NF-κB, in turn conferring a degree of apoptosis suppression, NF-κB mediated apoptosis suppression might also contribute to the MCR phenotype of V79 MCS. Oloumi et al. (2002) observed the up-regulation of *B-ind 1* in MCS cultures, the product of which potentiates activation of NF-κB via Rac1 (Courilleau et al. 2000).

The third differentially regulated gene for which links to MCR can be drawn is *p48*. Up-regulated 4.4-fold in MCS, this interferon stimulated transcription factor is also involved in global genomic

repair (Hwang et al. 1999; Luker et al. 2001). Luker et al. (2001) demonstrated that over-expression of *p48* in breast cancer derived cell lines imparts resistance to anti-microtubule agents. Several other IFN related genes were also up-regulated in paclitaxel resistant cells, and this resistant phenotype was independent of IFN signalling.

Luker et al. (2001) conclude that *p48* is responsible for the IFN independent regulation of downstream IFN-responsive genes, but were unable to identify the mechanism of *p48* activation. They do however note that over-expression of IFN-inducible genes has been identified in confluent human mammary epithelial cells, but not proliferating cultures (Perou et al. 1999). The simplest explanation for this observation is induction of down-stream IFN response genes by STAT1, which was also up-regulated (Perou et al. 1999). In HCT116 MCS we also observe the up-regulation of STAT1 (1.8-fold by real-time PCR) and a group of 11 other IFN inducible genes, including *p48*.

While STAT1 is best recognised for its role in IFN signalling, the observations of Perou et al. (1999) and pattern of differential expression in tumours (Arany et al. 2003), suggests a relationship to state of differentiation. Similarly, a number of the IFN related genes identified in our study are also indicators of differentiation, as are a number of genes for which expression varies in tumours. This is consistent with the widely held view that cells cultivated as MCS are more differentiated than those cultivated as monolayers.

In a more general sense, the identification of 42 differentially regulated genes demonstrates that the extent to which such changes occur in 3D culture is greater than previously reported, and that differential regulation of multiple genes in any given case may well contribute to the overall MCR phenotype. The three resistance related genes identified here, also suggest that different modes of resistance might exist for any given case, in this instance via modulation of intracellular calcium levels, apoptosis suppression, and enhanced DNA damage repair.

These findings relate specifically to the colon carcinoma cell line HCT116. Further microarray based studies using other cell lines may give a clearer understanding of common changes occurring in gene expression and/or reveal tumour-type related trends and additional MCR related genes. Similarly functional studies directly examining the action of the identified genes (e.g. knockout/RNAi) will firmly establish if they are indeed mediators of the MCR phenotype.

Acknowledgements

We gratefully acknowledge the SRC for Functional and Applied Genomics Microarray Facility for provision of the arrays. N.T. thanks Frances Harding (Chemical Engineering, University of Queensland) for her help with regards to real-time PCR.

References

Arany, I., Chen S.H., Megyesi J.K., Adler-Storthz K., Chen Z., Rajaraman S., Ember I.A., Tyring S.K. and Brysk M.M. 2003. Differentiation-dependent expression of signal transducers and activators of transcription (STATs) might modify responses to growth factors in the cancers of the head and neck. Cancer Lett. 199(1): 83–89.

Baldwin A.S. 2001. Control of oncogenesis and cancer therapy resistance by the transcription factor NF-kappa B. J. Clin. Invest. 107(3): 241–246.

Courilleau D., Chastre E., Sabbah M., Redeuilh G., Atfi A. and Mester J. 2000. B-ind1, a novel mediator of Rac1 signaling cloned from sodium butyrate-treated fibroblasts. J. Biol. Chem. 275(23): 17344–17348.

Debatin K.M. 2004. Apoptosis pathways in cancer and cancer therapy. Cancer Immunol. Immunother 53(3): 153–159.

Desoize B. and Jardillier J. 2000. Multicellular resistance: a paradigm for clinical resistance? Crit. Rev. Oncol. Hematol. 36(2–3): 193–207.

Dubessy C., Merlin J.M., Marchal C. and Guillemin F. 2000. Spheroids in radiobiology and photodynamic therapy. Crit. Rev. Oncol. Hematol. 36(2–3): 179–192.

Flatmark K., Pedersen K., Nesland J., Rasmussen H., Aamodt G., Mikalsen S., Bjornland K., Fodstad O. and Maelandsmo G. 2003. Nuclear localization of the metastasis-related protein s100a4 correlates with tumour stage in colorectal cancer. J. Pathol. 200(5): 589–595.

Fracasso G. and Colombatti M. 2000. Effect of therapeutic macromolecules in spheroids. Crit. Rev. Oncol. Hematol. 36(2–3): 159–178.

Hamilton G. 1998. Multicellular spheroids as an in vitro tumor model. Cancer Lett. 131: 29–34.

Huang J., Teng L., Liu T., Li L., Chen D., Li F., Xu L.G., Zhai Z. and Shu H.B. 2003. Identification of a novel serine/threonine kinase that inhibits TNF-induced NF-kappaB activation and p53-induced transcription. Biochem. Biophys. Res. Commun. 309(4): 774–778.

Hwang B.J., Ford J.M., Hanawalt P.C. and Chu G. 1999. Expression of the p48 xeroderma pigmentosum gene is p53-dependent and is involved in global genomic repair. Proc. Natl. Acad. Sci. USA 96(2): 424–428.

Kelm J.M., Timmins N.E., Brown C.J., Fussenegger M. and Nielsen L.K. 2003. Method for generation of homogeneous multicellular tumor spheroids applicable to a wide variety of cell types. Biotechnol. Bioeng. 83(2): 173–180.

Knowles H.J. and Phillips R.M. 2001. Identification of differentially expressed genes in experimental models of the tumor microenvironment using differential display. Anticancer Res. 21(4A): 2305–2311.

Kunz-Schughart L. and Mueller-Klieser W. 2000. Three-dimensional culture. In: Masters J. (ed.), Animal Cell Culture: A Practical Approach. 3rd ed. Oxford University Press, New York, pp. 123–184.

Kunz-Schughart L.A., Kreutz M. and Knuechel R. 1998. Multicellular spheroids: a three-dimensional *in vitro* culture system to study tumour biology. Int. J. Exp. Pathol. 79(1): 1–23.

Lazareff J.A., Suwinski R., De Rosa R. and Olmstead C.E. 1999. Tumor volume and growth kinetics in hypothalamic-chiasmatic pediatric low grade gliomas. Pediatr. Neurosurg. 30(6): 312–319.

Luker K., Pica C., Schreiber R. and Piwnica-Worms D. 2001. Overexpression of irf9 confers resistance to antimicrotubule agents in breast cancer cells. Cancer Res. 61(17): 6540–6547.

Marusic M., Bajzer Z., Vuk-Pavlovic and Freyer J. 1994. Tumour growth *in vivo* and as multicellular spheroids compared by mathematical models. Bull. Math. Biol. 56: 617–631.

Mayo M.W. and Baldwin A.S. 2000. The transcription factor NF-kappaB: control of oncogenesis and cancer therapy resistance. Biochim. Biophys. Acta 1470(2): M55–62.

Moriyama-Kita M., Endo Y., Yonemura Y., Heizmann C., Schafer B., Sasaki T. and Yamamoto E. 2004. Correlation of s100a4 expression with invasion and metastasis in oral squamous cell carcinoma. Oral Oncol. 40(5): 496–500.

Mueller-Klieser W. 1997. Three-dimensional cell cultures: from molecular mechanisms to clinical applications. Am. J. Physiol. 273(4 Pt 1): C1109–1123.

Nederman T. and Twentyman P. 1984. Spheroids for studies of drug effects. Recent Results Cancer Res. 95: 84–102.

Olive P.L. and Durand R.E. 1994. Drug and radiation resistance in spheroids: cell contact and kinetics. Cancer Metastasis Rev. 13(2): 121–138.

Olive P.L., Banath J.P. and Evans H.H. 1993. Cell killing and DNA damage by etoposide in Chinese hamster V79 monolayers and spheroids: influence of growth kinetics, growth environment and DNA packaging. Br. J. Cancer 67(3): 522–530.

Oloumi A., MacPhail S.H., Johnston P.J., Banath J.P. and Olive P.L. 2000. Changes in subcellular distribution of topoisomerase IIalpha correlate with etoposide resistance in multicell spheroids and xenograft tumors. Cancer Res. 60(20): 5747–5753.

Oloumi A., Lam W., Banath J.P. and Olive P.L. 2002. Identification of genes differentially expressed in v79 cells grown as multicell spheroids. Int. J. Radiation Biol. 78(6): 483–492.

Perou C.M., Jeffrey S.S., van de Rijn M., Rees C.A., Eisen M.B., Ross D.T., Pergamenschikov A., Williams C.F., Zhu S.X., Lee J.C., Lashkari D., Shalon D., Brown P.O. and Botstein D. 1999. Distinctive gene expression patterns in human mammary epithelial cells and breast cancers. Proc. Natl. Acad. Sci. USA 96(16): 9212–9217.

Poland J., Sinha P., Siegert A., Schnolzer M., Korf U. and Hauptmann S. 2002. Comparison of protein expression profiles between monolayer and spheroid cell culture of ht-29 cells revealed fragmentation of ck18 in three-dimensional cell culture. Electrophoresis 23(78): 1174–1184.

Rainaldi G., Calcabrini A., Arancia G. and Santini M.T. 1999. Differential expression of adhesion molecules (CD44, ICAM-1 and LFA-3) in cancer cells grown in monolayer or as multicellular spheroids. Anticancer Res. 19(3A): 1769–1778.

Ramakers C., Ruijter J.M., Deprez R.H. and Moorman A.F. 2003. Assumptionfree analysis of quantitative real-time polymerase chain reaction (PCR) data. Neurosci. Lett. 339(1): 62–66.

Rosty C., Ueki T., Argani P., Jansen M., Yeo C., Cameron J., Hruban R. and Goggins M. 2002. Overexpression of S100A4 in pancreatic ductal adenocarcinomas is associated with poor differentiation and dna hypomethylation. Am. J. Pathol. 160(1): 45–50.

Shiras A., Bhosale A., Patekar A., Shepal V. and Shastry P. 2002. Differential expression of CD44(S) and variant isoforms v3, v10 in three-dimensional cultures of mouse melanoma cell lines. Clin. Exp. Metastasis 19(5): 445–455.

Sutherland R. 1988. Cell and environment interactions in tumor microregions: the multicell spheroids model. Science 240: 177–184.

Wartenberg M., Frey C., Diedershagen H., Ritgen J., Hescheler J. and Sauer H. 1998. Development of an intrinsic P-glycoprotein-mediated doxorubicin resistance in quiescent cell layers of large, multicellular prostate tumor spheroids. Int. J. Cancer 75(6): 855–863.

Weaver V.M., Lelievre S., Lakins J.N., Chrenek M.A., Jones J.C., Giancotti F., Werb Z. and Bissell M.J. 2002. Beta4 integrin-dependent formation of polarized three-dimensional architecture confers resistance to apoptosis in normal and malignant mammary epithelium. Cancer Cell 2(3): 205–216.

Wu M., Xu L.G., Zhai Z. and Shu H.B. 2003. SINK is a p65-interacting negative regulator of NF-kappaB-dependent transcription. J. Biol. Chem. 278(29): 27072–27079.